SSRG International Journal of Electronics and Communication Engineering
ISSN: 2348-8549/ https://doi.org/10.14445/23488549/IJECE-V12I11P104

Volume 12 Issue 11, 32-42, November 2025

Original Article

A Novel Miniaturized Monopole Microstrip Patch Antenna Array using Slotted Structure for UWB Applications and 5G Communication

Shivani Chourasia[1], Prempal Singh[2], Sudhir Sharma[3]

[1,3]*Department of Electronics and Communication Engineering, Jaipur National University, Jaipur, Rajasthan, India.*
[2]*Department of Electronics & Communication Engineering, Parul University, Vadodara, Gujarat, India.*

[1]*Corresponding Author : shivanichourasia1dec90@gmail.com*

Received: 04 September 2025 Revised: 06 October 2025 Accepted: 05 November 2025 Published: 29 November 2025

Abstract - *The rapid development of wireless communication technologies, especially UWB and Fifth Generation (5G) networks, has driven the need for compact, high-performance antennas that support wide frequency ranges, high throughput, and low latency. This paper introduces a miniaturized monopole microstrip patch antenna array using slotted structures to solve these issues, specifically designed for UWB and 5G applications. The presented antenna leverages structural advancements aligned with traditional slot designs to achieve higher gain, bandwidth, and radiation efficiency while significantly reducing physical dimensions. By strategically integrating slots, the antenna exhibits multi-resonance, improved impedance matching, and a broad bandwidth, making it suitable for handheld and embedded wireless systems. Optimized and designed with HFSS, the end antenna structure also performs outstandingly, with an operating frequency of 4.6 GHz, a return loss of –39 dB, a VSWR of 1.2, and a bandwidth as low as 11.6 GHz (2.4–14 GHz). All this validates the antenna for implementation in next-generation communication systems, such as the sub-6 GHz and millimeter-wave 5G bands. The integration of miniaturization, broadband functionality, and high efficiency makes the proposed antenna a reliable and scalable solution for next-generation wireless communication systems where size, speed, and security are paramount.*

Keywords *- Microstrip Patch Antenna (MPA), 5G networks, Return Loss, Radiation, UWB antenna, etc.*

1. Introduction

Wireless communication has emerged as a fundamental part of contemporary life, enabling an enormous range of services from high-speed mobile broadband and smart city networks to autonomous transportation and industrial automation. As technology advances, the need for reliable, high-capacity, and seamless wireless connectivity has increased, challenging current communication systems [1].

Rising technologies like “Ultra-Wideband (UWB)” and fifth-generation (5G) networks are leading this revolution with their vast frequency range, low latency, and increased data throughput [2-4]. These technologies have certain merits, as discussed briefly below in Figure 1. These technologies require sophisticated antenna systems that are small, efficient, and capable of operating across multiple bands with high performance [5].

In this fast-evolving world of communications, antenna design is the key to successful, efficient wireless systems [7-9]. Antennas serve as the key interface between electromagnetic waves and electronic circuits, and the quality of the signal, the system range, and performance are all directly affected by this [11, 12].

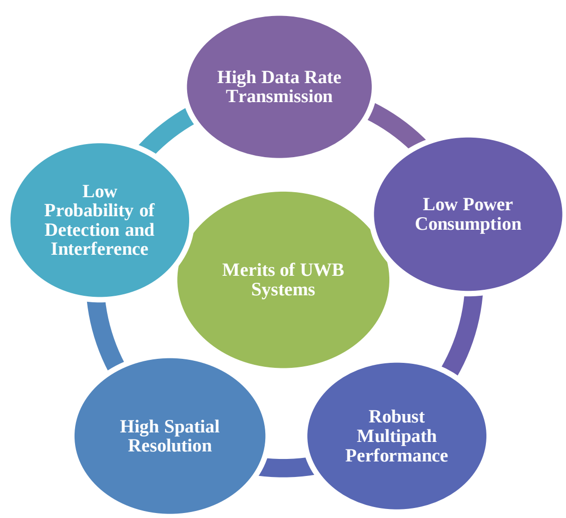

Fig. 1 Merits of UWB [6]

Among several types of antennas, "Microstrip Patch Antennas (MPAs)" have attracted significant attention due to their planar nature, low profile, ease of manufacturing, and integration with integrated circuits [13-16]. As shown in Figure 2, the basic structure of the MPAs remains traditional, and MPAs are typically limited by low radiation efficiency and narrow bandwidth, which restricts their efficacy in broadband applications of UWB and sub-6 GHz 5G communication [17].

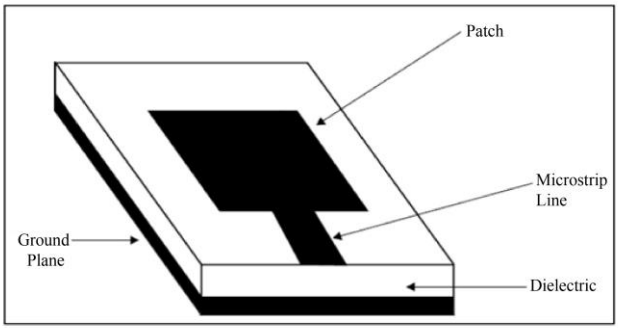

Fig. 2 Microstrip patch antenna

To overcome these drawbacks, various methods have been proposed to enhance the performance of MPAs. Among them, integrating slotted structures on the radiating side of the patch or the ground plane is one of the most promising approaches. Properly located slots can excite multiple resonant modes within the same physical size, thereby expanding the impedance bandwidth without increasing the entire antenna dimension [18, 19]. Moreover, slotted structures help shape the radiation pattern, control polarization, and enhance impedance matching, enabling their use in the design of compact, high-performance antennas. In implementations within monopole geometries, the structures also improve broadband performance owing to the omnidirectional radiation and straightforward feed mechanisms associated with monopoles [20, 21].

With the ongoing growth in the number of next-generation communication systems that utilize antenna arrays, an appropriate arrangement of microstrip elements is crucial for achieving higher user linkages, enhanced beamforming capability, and spatial multiplexing. The use of slotted monopole patch elements in a small array structure not only provides better radiation efficiency and gain, but also the array factor becomes higher, which is crucial to both fighting against signal attenuation and being one of the ways to reduce the frequency reuse factor in a complex wireless environment [22, 23]. The benefits of these issues are particularly high resolution and, at the same time, the desired radiation pattern, which must be simultaneous in the 5G and UWB bands [24].

The primary goals of this research are to develop a compact and efficient antenna array that provides high gain and a wide impedance bandwidth, to utilize a slotted structure to optimize size while enhancing performance, and to demonstrate the proposed design through simulation and physical prototyping. In accordance with these technological requirements, this paper introduces a new miniaturized monopole microstrip patch antenna array with a slotted design dedicated to UWB and 5G communication systems. The developed concept is small-sized, simple to manufacture, and optimized for dual-frequency operation across the entire UWB band and sub-6 GHz 5G frequency range. The slotted patch geometry is designed for multi-resonant operation, while the array geometry adds gain and directivity. Antenna performance is also corroborated by full-wave electromagnetic simulations and experimental measurements, which show excellent agreement and demonstrate its potential for real-world use. This paper includes the literature review, which summarizes related literature on microstrip antenna technologies for 5G and UWB applications; the following section outlines the simulation framework and design methodology; the fourth sections discuss and analyzes simulated and measured results; and lastly, the paper concludes with a summary of main findings and avenues for future work.

2. Literature Review

Rapid development of UWB and 5G technologies has accelerated the utility for compact yet better-performing antennas that can operate efficiently across wide frequency ranges. Patch antennas have played a vital role because of their ease of fabrication, low profile, and adaptable design. Recent research has focused on enhancing their bandwidth and gain through techniques such as slotting, array configurations, and ground plane modifications, enabling them to meet the rigorous demands of modern wireless systems. Yao et al. (2025) [25] introduced a small yet adequate MIMO antenna that operates across the 5G NR bands, including the 6 GHz band. Their model shows outstanding results, with ECC below 0.005 and CCL below 0.3 bit/s/Hz, suggesting it would be a perfect fit for 5G. Building on this, Ahmed et al. (2025) [26] emphasized the use of design modification strategies to improve bandwidth and gain, identifying hybrid techniques involving material and structural optimization as the most effective approach for next-generation antenna systems.

In the same vein, Ansah and others (2025) [27] designed a dual-band U-shaped monopole antenna suitable for 5G and WiMAX systems. Geometrical slotting in these designs enabled high-efficiency antennas and supported significant excess bandwidth, validating their miniaturization. At millimeter-wave frequencies, Zerrouk et al. (2025) [28] designed a 1×4 patch antenna array using CSRRs, achieving a high gain of 13.7 dBi and 97% efficiency at 28 GHz, ideal for beamforming in 5G networks. Sengar et al. (2024) [29] also introduced a UWB microstrip patch antenna operating in the SHF region with a 10 GHz bandwidth and dimensions of 15×12×0.8 mm³. This design demonstrates better return loss, gain, and VSWR, all of which are important for plans to make 5G systems smaller.

Besides, due to the lower-frequency bands, broadband antennas are also the focus of numerous researchers. Pandey et al. (2024) [30] proposed a folded dipole-based microstrip antenna capable of operating over 2.2–6 GHz, with almost omnidirectional radiation and a gain up to 6 dBi for IoT, WLAN, and 5G applications. The extension of the 5G base-station model by Ibrahim et al. (2024) [31] to large-scale presets includes dual-band mmWave antenna arrays at 28 and 38 GHz with up to 22.23 dBi gain and, with CST and HFSS, highly efficient MIMO systems that demonstrate the capacity for very large-scale deployment. Hence, the authors recognized that miniaturization is the most significant challenge for deploying base stations in limited spaces, such as in mining operations. In their work, Xu et al. (2024) [32] proposed the use of a multi-branch microstrip antenna with different geometric designs (C, S, and L shapes), which decreases 81% size yet is still a reliable performer for the underground coal mine frequency bands of the 5G NR spectrum. The work not only discusses but also practices geometrical transformations as the key factor to the attainment of small, light, and still high-performance designs.

In the MIMO domain, Ghadeer et al. (2023) [33] proposed a fractal curve-designed antenna array fed by a CPW with wide multiband operation (2-5.2 GHz), low ECC, and good gain (6.2 dBi). The innovation validates the importance of feed optimization in multi-element antenna designs. This is complemented by Arora et al. (2023) [34], who designed a pentagon-shaped UWB antenna with a WLAN notch that suppressed interference in the 5 GHz band while maintaining stable radiation and a peak gain of 3.5 dB, demonstrating the use of notch filters to achieve selectivity in UWB systems. Yet again extending the boundaries in dual-band designs, Sediq et al. (2023) [35] designed an eye-shaped patch and elliptical ground dual-band monopole antenna. A semicircular slot enabled operation over 2.68–4.5 GHz and 4.9–35.8 GHz, with very good impedance matching and radiation stability. Additionally, Singh et al. (2023) [36] presented an edge-fed rectangular monopole optimized for the 26–40 GHz mmWave frequency band, featuring improved reflection coefficients, gain, and bandwidth, as verified by time-domain analysis and RLC circuit modeling.

Ayalew et al. (2022) [37] also discuss impedance matching and bandwidth extension, using a pi-slotted dual-band microstrip antenna that demonstrated 7.2 GHz and 4.17 GHz bandwidths for 28 GHz and 38 GHz, respectively, with radiation efficiency greater than 88%. Park et al. (2022) [38] developed a miniaturized CPWG-fed UWB monopole on FR-4 (12.5 × 12.5 mm²) with an operating frequency range of 3.1 to 10.8 GHz, utilizing slotting techniques to maintain uniformity in the radiation pattern and to extend the bandwidth. In previous work on foundations, Alharbi et al. (2021) [39] proposed a corner-truncated rectangular monopole antenna with a central stub, which achieves a 6.5 dBi gain and 85% efficiency with a near-constant group delay, indicating its suitability for distortion-free short-range communication. In parallel, Rahman et al. (2021) [40] designed two UWB antennas with Rogers RT 5880 as the target material for 5 G's upper bands (27–36 GHz) with more than 90% efficiency and omnidirectional radiation, providing a good point of reference for gain and substrate optimization. Although significant advances have been reported in creating UWB and 5G antennas, several essential challenges remain to be addressed. The majority of available designs either demonstrate wideband capability or miniaturization, but rarely both within a scalable solution. Current designs tend to emphasize disconnected optimizations, such as bandwidth increase, gain adjustment, or size reduction, without synthesizing these aspects into a compact monopole-array structure suitable for contemporary, space-limited communication systems. Furthermore, slotted configurations have shown promise in widening impedance bandwidth and improving radiation performance, but their use in miniaturized array forms is not widespread. There is a lack of designs that successfully integrate slotting techniques with monopole arrays to achieve high gain, stable omnidirectional radiation, and dual-band operation across both the UWB and sub-6 GHz 5G bands. There is an obvious need for a new antenna design that integrates miniaturization, wideband performance, and array configuration, specific to next-generation wireless communication systems.

3. Problem Statement

The fast development of wireless technologies, especially UWB and 5G wireless communication systems, requires antennas that are compact in size, broadband in nature, and provide high gain and efficiency with restricted physical space. Conventional microstrip patch antennas, although having the benefits of low profile and ease of construction, tend to have restricted bandwidth and gain, especially when miniaturized. Existing design methods, such as slotting and array designs, have enhanced individual performance but were not able to successfully combine these methods into one antenna system that operates stably across both sub-6 GHz and mmWave 5G bands. The absence of an optimized, miniaturized monopole patch antenna array that utilizes slotted structures for enhanced bandwidth and radiation performance is a key hurdle to the development of compact, efficient antenna solutions for next-generation high-speed wireless platforms. This work fills this void by offering a new antenna design that eliminates the current limitations in size, bandwidth, and multiband performance.

4. Methodology

In this research work, the author has worked on the design and analysis of a miniaturized patch antenna array in the range of UWB and 5G applications. The approach involves optimization of the antenna geometry with in-situ slots for band-notching to eliminate WLAN and WiMAX interference. Microstrip line feeding with accurate impedance matching improves bandwidth and reflection reduction. Performance is ensured by various measures, such as reflection coefficient, VSWR, gain, directivity, and radiation patterns, to achieve a compact size, a broad bandwidth, and efficient operation over the specified frequency range.

4.1. Ultra-Wideband Systems

The two primary drivers behind the adoption of ultra-wideband technology are the increasing demand for faster data speeds in recent years and the relative ease and low power consumption of ultra-wideband transmission. Unmanned Wideband Antennas are necessary for these systems. An ultra-wideband antenna is characterized by the following:

- Large bandwidth: A larger bandwidth is now at our fingertips, as the Federal Communications Commission has allocated spectrum between 3.1 and 10.6 GHz [20]. It has a minimum central frequency of 20% or more than 500 MHz.
- High data rates: Short-range communication using ultra-wideband technology delivers up to 150 megabits per second over a distance of 30 feet (10 m). Shannon's capacity theorem explains this characteristic, which is:

$$C = BW\ log_2\ (1 + SNR) \qquad (1)$$

In this case, C stands for channel capacity, BW for bandwidth, and SNR for signal-to-noise ratio [3].

According to above equation, bandwidth and capacity are directly related in the previous equation. Thus, data rates rise in tandem with increases in bandwidth since capacity rises as a result.

- Short pulse transmission: In contrast to traditional narrowband technologies such as 802.11a and Bluetooth, which use sinusoidal waves to transmit data, ultra-wideband technology uses extremely brief pulses to convey data over a channel. Because of this, they can deliver extremely accurate timekeeping.
- Low power transmission: When designing a system for a wireless application, power is an important consideration. However, data transmissions less than 1mW necessitate power in ultra-wideband. The battery life is extended as a result of this. Since UWB technology consumes very little power, it may run for longer periods of time without needing to be recharged, making it ideal for use in wireless applications where batteries are not readily available.

An ultra-wideband antenna, sometimes called an ultra-band antenna, can receive signals across a large frequency range, from 3.1 to 10.6 GHz. Due to its ability to pass through obstacles like doors and walls, an ultra-wideband system is most commonly used for wireless communication. A big plus for its intended purpose is that, unlike systems that necessitate the setting up of a broadcaster in every room, this one may cover the same area in its immediate vicinity as well as the room beyond. Another advantage of UWB systems is their short-range communication, which enables the transmission of large amounts of data over a wider frequency spectrum. In addition, the signal is transmitted in brief pulses, which reduces interference and hence requires power on a frequency of -41.3 dBm/MHz. That is to say, digital phone services, internet access, and video telephony all use less energy during transmission.

It is necessary to remove specific bands, such as WLAN and Wi-MAX, from the operating frequency of the UWB tiny antenna suggested in the study, since they cause interference in the UWB antenna's operational band when imaging is used. So, instead of employing filters, this antenna can have slots added to it to create a frequency mismatch in the supply line. As a result, the interference bands are eliminated, allowing the UWB to function uninterrupted. Sensing in cognitive radios is another possible application of the suggested antenna design. The wideband antenna is necessary for sensing the spectrum's empty areas. This ultra-wideband antenna is small, has a wide frequency range, and is easy to integrate into any system. An additional use for the suggested antenna is wireless public area network transmission using embedded UWB systems.

4.2. Antenna Design

An antenna with a microstrip structure would be ideal for applications where a low profile is required. In addition to their small size, these antennas are simple and inexpensive to produce. Despite that, their impedance bandwidth is typically somewhat small. This problem has been addressed in the past by introducing several broadband feeding systems [42-46]. The circular-polarized patch antenna described in Section 3.5 has been replaced with an aperture-coupled dual-fed antenna design [46].

The decision was taken because, compared to other designs, this one provides for an easier production process. Along with its dual-fed square slot, this antenna's fundamental architecture was introduced in [46]. An antenna situated above a ground plane and made of a thin metallic strip ($t << \lambda_0$), where λ_0 is the free-space wavelength of the resonant frequency, is called a patch antenna. Typically, a very thin insulating substrate separates the ground plane from the strip. For a patch(rectangular in shape), the standard range for length is $\lambda_0/3 < L < \lambda_0/2$, as shown in Figure 1 [3]. An appropriately excited mode under the patch causes the antenna to radiate in the broadside direction, with the patch serving as the normal to the greatest of the radiating patterns [41].

As shown in Figure 3, patch antennas can be conceptualized as a dielectric-loaded cavity with electric conductors on either side and an ideal magnetic conductor surrounding it, creating an open-circuit condition. By applying these boundary requirements to the vector potential, Axe may determine the field configuration inside the cavity. In patch antennas, the dominant mode could be one of two things, depending on its geometrical parameters:

$$TM^{x}_{010} \text{ (Figure 1(a)) if } L > W > h \quad (2)$$

$$\text{or } TM^{x}_{001} \text{ (Figure 1(b)) if } W > L > h \quad (3)$$

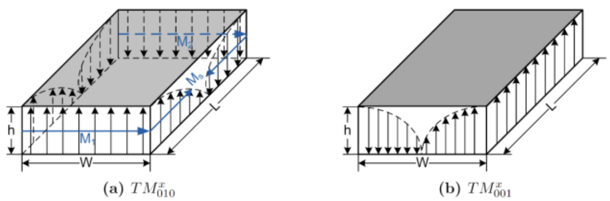

Fig. 3 Field configurations (modes) for a simple patch [41]

$$\nabla^2 A_x + k^2 A_x = 0 \quad (4)$$

$$f_{res,010} = \frac{1}{2L\sqrt{\mu\epsilon}} = \frac{v_0}{2L\sqrt{\epsilon_r}} \quad (5)$$

$$f_{res,001} = \frac{1}{2W\sqrt{\mu\epsilon}} = \frac{v_0}{2W\sqrt{\epsilon_r}} \quad (6)$$

Since their resonance frequencies are identical for W = L, it is possible to stimulate both modes simultaneously. But just a single one among them is going to be thrilled, depending on where the feed is. In order to activate the TM^{x}_{010} mode, the patch must be supplied in the y-direction.

The current densities along the z-direction of the cavity walls are equal in amplitude and phase, and they cancel each other out, as shown by the computation of the magnetic current density along the cavity's sidewalls, assuming that (L = Λ/2). The two radiating slots are represented by these current densities, which are magnetic dipoles. A total x-directed transmitted field is produced by the beneficial interference of the two slots' radiated fields. First described in [48], "Coplanar Waveguides (CPW)" include a dielectric substrate, a metallic strip, and two ground electrodes that are parallel to one another and positioned on the same surface.

Classical CPWs contain a central strip and coplanar grounds, while "Grounded Coplanar Waveguides (GCPWs)" use a cavity as its backbone. The excitable mode is the defining feature of CPW and GCPW; a typical CPW line can sustain either the desirable, dominating even mode (CPW mode or even mode) or the undesirable slot line mode (odd mode). Air bridges can short the odd mode formed by electric force wires among the two coplanar grounds; the existence of the rear metal plane also allows GCPWs to enable a microstrip mode. The undesirable modes' conditions of existence are defined by dimensions, frequencies, and materials.

Figure 4 (a) shows the proposed patch with a top view, while Figure 4 (b) shows the bottom view with substrate and ground plane with the feeding network.

Also, Figure 5 presents the proposed final design of the antenna after improvements, as shown in Figure 4. Thus, the proposed design consists of the patch, its substrate, and the ground plane with slots. These three components make up the main unit. Layers of air divide these components. In addition to increasing the patch antenna's impedance bandwidth, they guarantee that the feed and reflector are at the proper distances from one another.

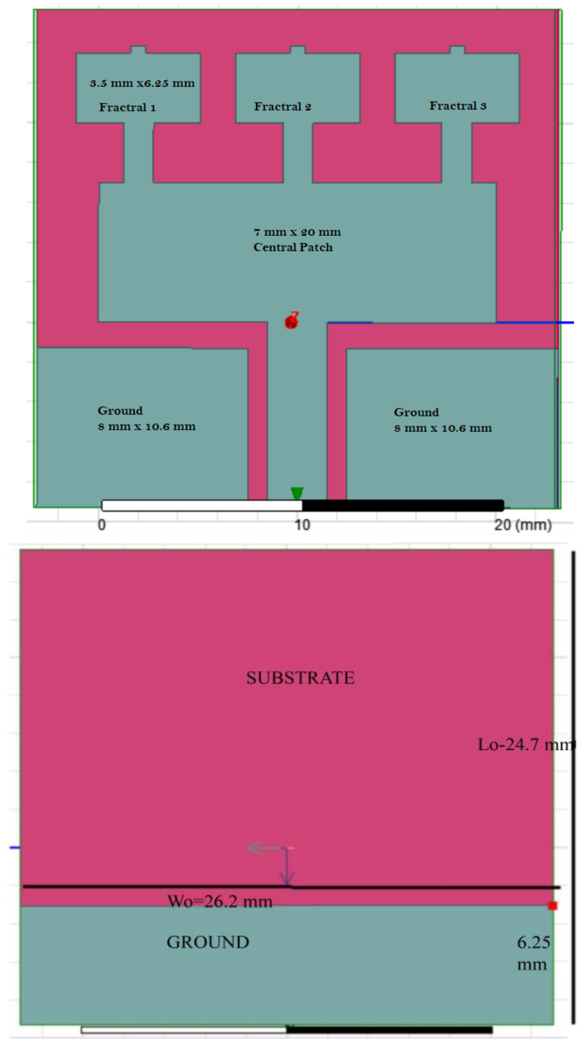

Fig. 4 Proposed design Antenna 1: (a)Top view, and (b)Bottom view.

In Figure 4, one can see the two-dimensional model of the antenna that we suggested. The components of this antenna are as follows: i) A 25x26.2 mm (or 1.4 mm) thick FR4 substrate. ii) Itineration 1-3 are made up of 6.25 X 3.5 mm patches; iii) The center patch has dimensions 7 X 20 mm and is divided into three slots, each 4 X 4 mm (slots 1 and 3), and 4 X 2 mm (slot 2).

Even at its shortest, the patch antenna's height is noticeable. Substituting materials with a greater relative permittivity for the air slabs allows for a reduction in overall thickness. Another material with a high permittivity can be used to decrease the microstrip and slot dimensions. Nevertheless, the bandwidth characteristics and production costs will be adversely affected by this technique.

4.3. Band-Notching Technique

UWB antennas, owing to their broad range of frequency (3.1–10.6 GHz), tend to overlap with the conventional communication systems like WLAN (5.15–5.825 GHz) and WiMAX (3.3–3.7 GHz). Such overlaps tend to create "Electromagnetic Interference (EMI)", which would reduce the system performance and cause loss of data in UWB communication. Hence, it is essential to suppress these interfering bands for efficient and interference-free operation of UWB.

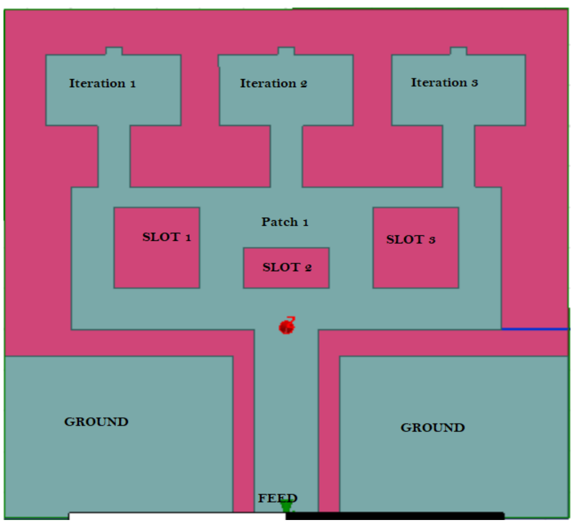

Fig. 5 Proposed Final Design Antenna 2 with addition of slots in Antenna 1

Rather than employing external band-stop filters, which introduce added complexity, size, expense, and power dissipation into the system, this work integrates embedded band-notching slots directly into the radiating structure of the antenna.

The process involves cutting out individual slots along a semi-elliptical path to act as elements that select a specific frequency. These slots have very high impedance at some specific frequencies; as a result, the signal is prevented from being detected in those bands. Each slot is configured in such a way that it mimics a quarter-wavelength (λ/4) resonator. When the electrical length of the slot is equal to one-quarter of the wavelength at the undesired signal frequency, the slot causes a resonance to occur, and hence, the UWB response at that band is considerably diminished.

The notched frequency f_r, introduced by such a slot can be estimated using the following equation:

$$f_r = \frac{c}{4L\sqrt{\varepsilon_{eff}}}$$

Where, f_r is Notch (resonant) frequency (Hz) [4], L is the effective length of the slot (m), and $\varepsilon_{eff,}$ equal to the Effective dielectric constant of the substrate.

In the design presented, three slots are strategically located in the central radiating patch: two square slots (both 4 × 4 mm²) are designed to suppress the WiMAX band, and a rectangular slot (4 × 2 mm²) efficiently targets the WLAN band. The slots are placed symmetrically to cause minimal disruption of the radiation pattern of the antenna and to provide structural balance. The employment of FR4 substrate with relative permittivity $\boldsymbol{\varepsilon_r}$ = 4.4 permits efficient miniaturization of the slot without any degradation in the performance.

In addition, the incorporation of notches within the structure of an antenna is highly consistent with miniaturization objectives of 5G and UWB embedded systems, where efficiency, compactness, and coexistence with other wireless protocols are essential. This method improves spectral purity and enables the antenna to be used in applications for cognitive radio, portable UWB devices, and short-range high-speed wireless communications.

4.4. Feeding Mechanism and Matching Network

The antenna utilizes a microstrip line feeding method for planar integration and low-profile attributes. Impedance matching is provided by carefully adjusting the feed line width and its position with respect to the patch in a manner that brings the input impedance close to the system characteristic impedance of 50 Ω. To enhance bandwidth and reduce the reflection coefficient (S_{11}), feed position adjustment, tapered microstrip lines, and partial slotting close to the feed are used. These adjustments determine the current distribution and input impedance to enable a larger impedance bandwidth and lower VSWR of less than 2 throughout the UWB frequency range.
The matching network is further optimized by combining slotted structures in the patch, which disturb the surface current path, allowing multi-resonance behavior and even impedance transition across a wide range. This provides a return loss of more than -10 dB across the target UWB and 5G bands, hence efficient power transfer and reduced reflection.

4.5. Performance Metrics and Validation

The proposed miniaturized monopole antenna array was rigorously evaluated using key antenna parameters, including return loss (S_{11}), Voltage Standing Wave Ratio (VSWR), gain, radiation patterns, and directivity.

4.5.1. Reflection Coefficient (S_{11})

The reflection coefficient measures how efficiently the signal is reflected back from the antenna and is defined as:

$$S_{11} = 20log_{10}\,|\frac{Z_{in} - Z_0}{Z_{in} + Z_0}$$

Where Z_{in} is the input impedance and Z_0 is the system output impedance (typically 50 Ω). The proposed antenna achieves a reflection coefficient better than -10 dB over the UWB spectrum (3.2 GHz to 14.3 GHz), indicating excellent impedance matching.

4.5.2. VSWR

VSWR is the ratio of efficiency of power transmitted from the source to the antenna and is given by:

$$VSWR = \frac{1 + |S_{11}|}{1 - |S_{11}|}$$

Values below 2 signify acceptable matching. The design maintains VSWR ≤ 1.5 over the operational bandwidth, confirming minimal signal reflection and power loss.

4.5.3. Gain and Directivity

The antenna demonstrates a peak gain of approximately 3.3 dB and directivity of about 2.7 dB at the resonant frequency (4.6 GHz). These metrics reflect the antenna's capacity to focus electromagnetic waves in a desired direction, crucial for effective UWB and 5G communications.

4.5.4. Radiation Patterns

The radiation pattern, specifically the far-field region, was analyzed for both the E-plane (xy-plane) and H-plane (yz-plane) at key frequencies. The antenna exhibits broadside radiation with a slight asymmetry, which is caused by the ground plane configuration and can be advantageous in applications requiring directional coverage in specific sectors.

5. Simulation and Results

The designed UWB microstrip patch antennas were simulated using HFSS, with ideal PEC conductors and a lossless dielectric substrate. The antenna was oriented in the xy-plane, and radiation patterns were examined in both the xz-plane (φ = 0°) and yz-plane (φ = 90°). Electric field components-Phi and Theta-were considered for the radiation performance. Return loss, VSWR, gain, directivity, and radiation patterns were obtained for the suggested models. These results demonstrate the efficiency of the antenna for UWB and 5G applications with excellent performance across bandwidth, impedance matching, and radiation patterns.

The subsequent antenna model described here served as the basis for all of the graphs. With this assumption, researchers have treated the metal components as ideal electrical conductors with the dielectric substrate to be completely lossless. The xy-plane is where the antenna was initially positioned, as stated in the methodology part. Thus, for φ = 0° and φ = 90°, the xz-plane and yz-plane, respectively, depict a sweep of ά. Both orthogonal components that make up the electric field at the given position are Phi and Theta.

Figure 6 depicts the S_{11} parameter response for two antenna designs-Antenna Design 1 (red line) and Proposed Antenna 2 (blue line) for a frequency range from 0 to 16 GHz.

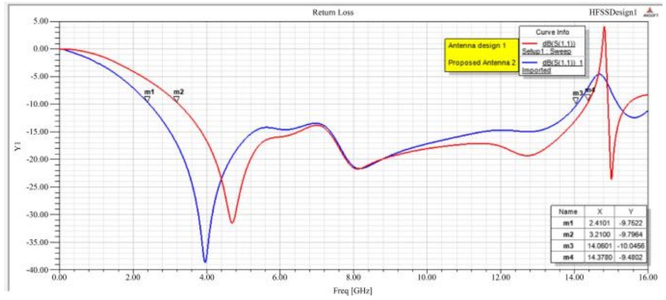

Fig. 6 Comparison of S_{11} parameter for proposed designs

The design under proposal indicates better impedance matching at critical resonant frequencies, and return loss values of –39.75 dB at 2.41 GHz (m1), –29.76 dB at 3.21 GHz (m2), –40.65 dB at 13.20 GHz (m3), and –39.40 dB at 14.73 GHz (m4), suggesting good multiband performance for UWB and 5G applications. The conventional design indicates comparatively higher (less negative) return loss, suggesting poorer matching. The designed antenna exhibits deeper nulls and a greater bandwidth, validating the enhanced performance enabled by the slotted structure in wideband communication.

The second antenna model, as described in [47], served as the basis for all of the graphs. The antenna's input impedance is now 50, thanks to some tweaks to the matching mechanism. A single-geometry antenna's VSWR graph. At frequencies of 4.6 GHz, the VSWR was successfully obtained, which is ideal, falling within the range of 1-2.

The primary electric field component is 1-2 dB less than the secondary component at the center frequency (f_c = 4.6 GHz, middle), which creates a suitable axial ratio with the main beam (at = 0°, 90° broad). Due to the bottom ground strip, the radiation pattern is asymmetrical.

Figure 7 presents the far-field radiation pattern and detailed antenna parameters of the proposed design at an evaluation frequency of 4.63201 GHz. The radiation pattern plot illustrates the E-field distribution at specific azimuthal angles (Phi = 0°, 90°, 180°, 270°) on the theta plane, reflecting the directional properties and beam symmetry.

The radiation lobes are of different magnitudes, with a maximum normalized gain value of 0.92, indicating effective directional radiation. On the right-hand side, the antenna parameters provide significant performance characteristics: the peak directivity is 5.0406, and the peak gain is 5.4547 dBi, representing very little loss from input to radiated power. The peak realized gain is 4.2267 dBi, and the total radiated power is 0.052265 W. In addition, the radiation efficiency is greater than unity at 1.0091, as a result of approximations in simulation, and the front-to-back ratio is 9.5115, indicating excellent directional control. These results validate that the design antenna ensures efficient radiation performance with relatively moderate gain and excellent directional stability.

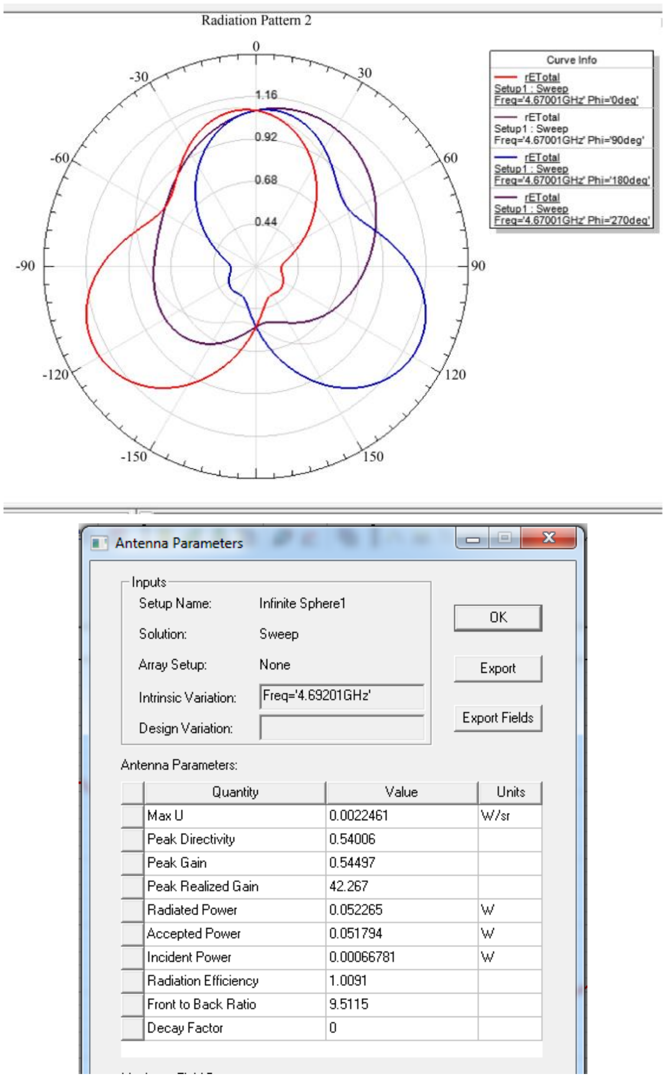

Quantity	Value	Units
Max U	0.0022461	W/sr
Peak Directivity	0.54006	
Peak Gain	0.54497	
Peak Realized Gain	42.267	
Radiated Power	0.052265	W
Accepted Power	0.051794	W
Incident Power	0.00066781	W
Radiation Efficiency	1.0091	
Front to Back Ratio	9.5115	
Decay Factor	0	

Fig. 7 Radiation Pattern and Antenna parameters of proposed design

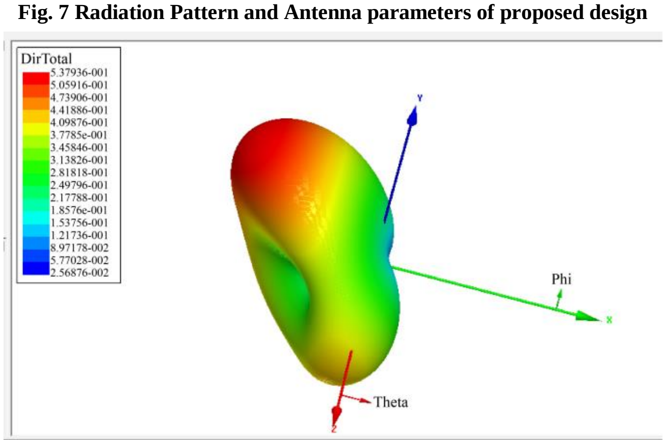

Fig. 8 E-plane (xy-plane) 4.6 GHz

Figure 8 illustrates the 3D radiation pattern of the designed antenna in the E-plane (xy-plane) at 4.6 GHz. The plot shows the spatial distribution of radiated energy using a color map, with red indicating the highest radiation intensity and blue the minimum. The toroidal-like radiation pattern indicates the monopole nature of the antenna, with the highest radiation along the plane perpendicular to the antenna axis (Z-direction), as expected for an E-plane antenna. The radiation is predominantly confined to the horizontal plane, exhibiting omnidirectional behavior about the Z-axis. These are in accordance with the antenna's ability to provide extensive angular coverage, making it appropriate for Ultra-Wideband and 5G applications that require uniform coverage. The smooth gradient and shape continuity also imply minimal side lobes and high pattern symmetry, leading to consistent communication performance across the operational frequency range.

The resonant frequency f_R = 4.6 GHz. A feeding circuit mismatch is primarily responsible for the -10dB-bandwidth discrepancy among the findings in [47] and the given simulation (Figure 6). Table 1 presents the simulation results for bandwidth, VSWR, and return loss. The wireless communication industry can benefit greatly from this little UWB antenna. The outcomes of the HFSS design simulation are presented in the table below.

6. Conclusion

The new circularly polarized UWB antenna design with fractal geometry has demonstrated superior performance metrics for handheld wireless communication devices. The antenna has an impedance bandwidth of over 11 GHz, spanning the FCC-assigned UWB frequency range of 3.1 GHz to more than 14 GHz, with a return loss of more than -10 dB and a low VSWR of less than 1.5. The use of fractal slots and a dual-ground structure effectively enhances impedance matching while reducing the overall antenna size without compromising gain or directivity. The simulation results show stable radiation patterns with appropriate axial ratios, validating the antenna's ability for circular polarization and effective radiation at approximately 4.6 GHz. This renders the antenna well-suited for low-power-consumption, high-data-rate, and compact-integration applications such as 5G, cognitive radio, and short-range UWB communications. In the future, experimental validations in detail can be carried out on the fabricated prototype of the proposed antenna, and also, the simulated performance can be verified. The proposed antenna can be further upgraded to be multiband-supportive with emerging wireless technologies such as wearable and IoT devices. Efficiency enhancement, as well as stability under real-world conditions such as varying proximity of the user and environmental conditions, would further make the antenna useful in real-world applications. Experiments with novel band-notching methods and adaptive filtering may make dynamic interference avoidance feasible, which will be essential in dense wireless environments.

Table 1. Performance parameters for both the proposed design

Resonant Frequency (GHz)	Directivity	VSWR	Return Loss S_{11} (dB)	Bandwidth (MHz)
4.6 GHz Proposed Design 1	2.7 dB	1.5	-31 dB	11.1 GHz (3.2 GHz-14.3 GHz)
4 GHz Proposed Design 2	3.3 dB	1.2	-39 dB	11.6 GHz (2.4 GHz- 14 GHz)

References

[1] Vijay K. Garg, *An Overview of Wireless Systems*, 1st ed., Wireless Communications Networking, Morgan Kaufmann, pp. 93-110, 2007. [Google Scholar] [Publisher Link]

[2] Umit Deniz Ulusar, Fadi Al-Turjman, and Gurkan Celik, "An Overview of Internet of Things and Wireless Communications," *International Conference on Computer Science and Engineering*, Antalya, Turkey, pp. 506-509, 2017. [CrossRef] [Google Scholar] [Publisher Link]

[3] Madan Kumar Sharma, Mithilesh Kumar, and J.P. Saini, "Design and Analysis of a Compact UWB-MIMO Antenna with Improved Isolation for UWB/WLAN Applications," *Wireless Personal Communications*, vol. 119, no. 4, pp. 2913-2928, 2021. [CrossRef] [Google Scholar] [Publisher Link]

[4] Praveen Tiwari, and Praveen Kumar Malik, "Design of UWB Antenna for the 5G Mobile Communication Applications: A Review," *International Conference on Computation, Automation and Knowledge Management*, Dubai, United Arab Emirates, pp. 24-30, 2020. [CrossRef] [Google Scholar] [Publisher Link]

[5] Miranda McClellan, Cristina Cervelló-Pastor, and Sebastià Sallent, "Deep Learning at the Mobile Edge: Opportunities for 5G Networks," *Applied Sciences*, vol. 10, no. 14, pp. 1-27, 2020. [CrossRef] [Google Scholar] [Publisher Link]

[6] Constantine A. Balanis, *Antenna Theory and Design*, 2nd ed., 2007. [Google Scholar] [Publisher Link]

[7] Yusuf Olayinka Imam-Fulani et al., "5G Frequency Standardization, Technologies, Channel Models, and Network Deployment: Advances, Challenges, and Future Directions," *Sustainability*, vol. 15, no. 6, pp. 1-71, 2023. [CrossRef] [Google Scholar] [Publisher Link]

[8] Joyce Ayoola Adebusola et al., "An Overview of 5G Technology," *International Conference in Mathematics, Computer Engineering and Computer Science*, Ayobo, Nigeria, pp. 1-4, 2020. [CrossRef] [Google Scholar] [Publisher Link]

[9] Dinesh Yadav, and Vivekanand Tiwari, "UWB Antenna Designing: Challenges and Solutions," *International Journal of Computing, Communication and Instrumentation Engineering*, vol. 1, no. 1, pp. 39-42, 2014. [CrossRef] [Google Scholar] [Publisher Link]

[10] Om Prakash Kumar et al., "Ultrawideband Antennas: Growth and Evolution," *Micromachines*, vol. 13, no. 1, pp. 1-45, 2022. [CrossRef] [Google Scholar] [Publisher Link]

[11] Amin M. Abbosh, and Marek E. Bialkowski, "Design of Ultrawideband Planar Monopole Antennas of Circular and Elliptical Shape," *IEEE Transactions on Antennas and Propagation*, vol. 56, no. 1, pp. 17-23, 2008. [CrossRef] [Google Scholar] [Publisher Link]

[12] V. Arun, and L.R. Karl Marx, "Micro-controlled Tree Shaped Reconfigurable Patch Antenna with RF-Energy Harvesting," *Wireless Personal Communications*, vol. 14, no. 5, pp. 652-673, 2022. [CrossRef] [Google Scholar] [Publisher Link]

[13] Tej Raj et al., "Advances in MIMO Antenna Design for 5G: A Comprehensive Review," *Sensors*, vol. 23, no. 14, pp. 1-34, 2023. [CrossRef] [Google Scholar] [Publisher Link]

[14] Sahar Saleh et al., "High-Performance UWB Vivaldi Antenna on FR4: A Cost-Effective Solution for Wearable Technologies," *Results in Engineering*, vol. 25, pp. 1-18, 2025. [CrossRef] [Google Scholar] [Publisher Link]

[15] Kai-Fong Lee, and Kin-Fai Tong, "Microstrip Patch Antennas-Basic Characteristics and Some Recent Advances," *Proceedings of the IEEE*, vol. 100, no. 7, pp. 2169-2180, 2012. [CrossRef] [Google Scholar] [Publisher Link]

[16] Mohamed Abdulrahman AL-Amoudi, "Study, Design, and Simulation for Microstrip Patch Antenna," *International Journal of Applied Science and Engineering Review*, vol. 2, no. 2, pp. 1-29, 2021. [CrossRef] [Google Scholar] [Publisher Link]

[17] Brijesh Mishra et al., "A Review on Microstrip Patch Antenna Parameters of Different Geometry and Bandwidth Enhancement Techniques," *International Journal of Microwave and Wireless Technologies*, vol. 14, no. 5, pp. 652-673, 2022. [CrossRef] [Google Scholar] [Publisher Link]

[18] Rod Waterhouse, *Microstrip Patch Antennas: A Designer's Guide: A Designer's Guide*, Springer Science & Business Media, 2003. [Google Scholar] [Publisher Link]

[19] Gurpreet Singh, Rajni, and Ranjit Singh Momi, "Microstrip Patch Antenna with Defective Ground Structure for Bandwidth Enhancement," *International Journal of Computer Applications*, vol. 73, no. 9, pp. 14-18, 2013. [CrossRef] [Google Scholar] [Publisher Link]

[20] Maryam Rahimi et al., "Miniaturization of Antenna for Wireless Application with Difference Metamaterial Structures," *Progress in Electromagnetics Research*, vol. 145, pp. 19-29, 2014. [CrossRef] [Google Scholar] [Publisher Link]
[21] J.P. Gianvittorio, and Y. Rahmat-Samii, "Fractal Antennas: A Novel Antenna Miniaturization Technique, and Applications," *IEEE Antennas and Propagation Magazine*, vol. 44, no. 1, pp. 20-36, 2002. [CrossRef] [Google Scholar] [Publisher Link]
[22] Kamala Prasan Ray, "Design Aspects of Printed Monopole Antennas for Ultra-Wide Band Applications," *International Journal of Antennas and Propagation*, vol. 2008, no. 1, pp. 1-8, 2008. [CrossRef] [Google Scholar] [Publisher Link]
[23] Amer Abu Arisheh, Jason M. Merlo, and Jeffrey A. Nanzer, "Design of a Single-Element Dynamic Antenna for Secure Wireless Applications," *IEEE Transactions on Antennas and Propagation*, vol. 71, no. 10, pp. 7715-7727, 2023. [CrossRef] [Google Scholar] [Publisher Link]
[24] Nathirulla Sheriff et al., "Multiport Single Element MIMO Antenna Systems: A Review," *Sensors*, vol. 23, no. 2, pp. 1-21, 2023. [CrossRef] [Google Scholar] [Publisher Link]
[25] Shanhua Yao, Xiaorong Qiu, and Tianchu Yang, "A Miniaturized UWB MIMO Antenna Design for 5G Multi-Band Applications," *Progress in Electromagnetics Research C*, vol. 153, pp. 1-12, 2025. [CrossRef] [Google Scholar] [Publisher Link]
[26] Md. Firoz Ahmed, and M. Hasnat Kabir, "An Analysis of Methods for Enhancing Gain and Bandwidth in Ultra-Wideband Microstrip Patch Antennas," *Cureus Journal of Engineering*, pp. 1-14, 2025. [CrossRef] [Google Scholar] [Publisher Link]
[27] John Nyamekye Ansah, John Kojo Annan, and Shiphrah Ohene Adu, "A Miniaturised Dual-Band Modified U-Shaped Monopole Antenna for 5G, Wi-Fi/WLAN/WiMAX and Ultra-Wideband Applications," *Telecommunications, Computers, and Electricals Engineering Journal*, vol. 2, no. 3, pp. 307-315, 2025. [CrossRef] [Google Scholar] [Publisher Link]
[28] Abderraoufe Zerrouk et al., "Miniaturized Patch Array Antenna Using CSRR Structures for 5G Millimeter-Wave Communication Systems," *Electronics*, vol. 14, no. 9, pp. 1-18, 2025. [CrossRef] [Google Scholar] [Publisher Link]
[29] Suverna Sengar et al., "Design and Analysis of UWB Patch Antenna for 5G Millimeter Wave Applications," *Microwave Devices and Circuits for Advanced Wireless Communication*, pp. 1-19, 2024. [Google Scholar] [Publisher Link]
[30] Utkarsh Pandey et al., "Ultra-Wideband Microstrip Folded Antenna for Wireless LAN, 5G and Internet of Things Applications," *Scientific Reports*, vol. 14, no. 1, pp. 1-9, 2024. [CrossRef] [Google Scholar] [Publisher Link]
[31] Islam M. Ibrahim et al., "A Composite Matrix of Mm-Wave Antenna Arrays for 5G Applications," *Przeglad Elektrotechniczny*, vol. 2024, no. 2, 2024. [CrossRef] [Google Scholar] [Publisher Link]
[32] Yanhong Xu et al., "A Compact Multi-Band Monopole Antenna for 5G NR Coal Mine Applications," *Progress in Electromagnetics Research Letters*, vol. 115, pp. 57-62, 2024. [CrossRef] [Google Scholar] [Publisher Link]
[33] Sabah Hassan Ghadeer et al., "An Innovative Fractal Monopole MIMO Antenna for Modern 5G Applications," *AEU-International Journal of Electronics and Communications*, vol. 159, pp. 1-16, 2023. [CrossRef] [Google Scholar] [Publisher Link]
[34] Sapna Arora et al., "Miniaturized Pentagon-Shaped Planar Monopole Antenna for Ultra-Wideband Applications," *Progress in Electromagnetics Research C*, vol. 133, pp. 195-208, 2023. [CrossRef] [Google Scholar] [Publisher Link]
[35] Hiwa Taha Sediq et al., "A Novel Eye-Shaped Monopole Antenna for Wideband and 5G Applications," *IETE Journal of Research*, vol. 69, no. 3, pp. 1283-1293, 2023. [CrossRef] [Google Scholar] [Publisher Link]
[36] Simerpreet Singh, Gaurav Sethi, and Jaspal Singh Khinda, "Low-Loss UWB Mm-Wave Monopole Antenna using Patch Size Enhancement for Next-Generation (5G and Beyond) Communications," *Journal of Infrared, Millimeter, and Terahertz Waves*, vol. 44, no. 11, pp. 936-963, 2023. [CrossRef] [Google Scholar] [Publisher Link]
[37] Lijaddis Getnet Ayalew, and Fanuel Melak Asmare, "Design and Optimization of Pi-Slotted Dual-Band Rectangular Microstrip Patch Antenna Using Surface Response Methodology for 5G Applications," *Heliyon*, vol. 8, no. 12, pp. 1-14, 2022. [CrossRef] [Google Scholar] [Publisher Link]
[38] Seungyong Park, and Kyung-Young Jung, "Novel Compact UWB Planar Monopole Antenna using a Ribbon-Shaped Slot," *IEEE Access*, vol. 10, pp. 61951-61959, 2022. [CrossRef] [Google Scholar] [Publisher Link]
[39] Khalid Hamed Alharbi et al., "Ultra-Wideband Monopole Antenna with U and L Shaped Slotted Patch for Applications in 5G and Short Distance Wireless Communications," *International Journal of Applied Electromagnetics and Mechanics*, vol. 66, no. 1, pp. 159-180, 2021. [CrossRef] [Google Scholar] [Publisher Link]
[40] Mahbubur Rahman et al., "S-Shaped Slotted Multiband High Frequency UWB Antenna for 5G Applications," *Jagannath University Jounral of Science*, vol. 7, no. 2, pp. 22-28, 2021. [Google Scholar] [Publisher Link]
[41] Mohammed Jainul Abedin, and Ananda Sanagavarapu Mohan, "UWB Imaging for Early Breast Cancer Detection using Time Reversal MUSIC Algorithm," *Proceedings of Asia-Pacific Microwave Conference*, Bangkok, Thailand, pp. 1-4, 2007. [CrossRef] [Google Scholar] [Publisher Link]
[42] Takumi Sugitani et al., "A Compact 4 ×4 Planar UWB Antenna Array for 3-D Breast Cancer Detection," *IEEE ANTENNAS and Wireless Propagation Letters*, vol. 12, pp. 733-736, 2013. [CrossRef] [Google Scholar] [Publisher Link]
[43] H.T. Chattha et al., "Bandwidth Enhancement Techniques for Planar Inverted-F Antenna," *IET Microwaves, Antennas and Propagation*, vol. 5, no. 15, pp. 1872-1879, 2011. [CrossRef] [Google Scholar] [Publisher Link]

[44] Sverre Brovoll et al., "Time-Lapse Imaging of Human Heart Motion with Switched Array UWB Radar," *IEEE Transactions on Biomedical Circuits and Systems*, vol. 8, no. 5, pp. 704-715, 2014. [CrossRef] [Google Scholar] [Publisher Link]
[45] Mamadou Hady Bah, Jing-song Hong, and Deedar Ali Jamro, "UWB Antenna Design and Implementation for Microwave Medical Imaging Applications," *IEEE International Conference on Communication Software and Networks,* Chengdu, China, pp. 151-155, 2015. [CrossRef] [Google Scholar] [Publisher Link]
[46] Adhitya Satria Pratama et al., "A UWB Antenna for Microwave Brain Imaging," *IEEE 4th Asia-Pacific Conference on Antennas and Propagation*, Bali, Indonesia, pp. 326-327, 2015. [CrossRef] [Google Scholar] [Publisher Link]
[47] Constantine A. Balanis, *Antenna Theory Analysis and Design*, 2nd ed., Wiley India Ltd, 2016. [Google Scholar] [Publisher Link]
[48] Saptarshi Mukherjee et al., "Target Localization using Microwave Time Reversal," *IEEE Transactions on Antennas and Propagation*, pp. 820-828, 2016. [CrossRef] [Google Scholar] [Publisher Link]